

# Full-resolution quality assessment for pansharpening

Giuseppe Scarpa, *Senior Member, IEEE*, Matteo Ciotola

**Abstract**—A reliable quality assessment procedure for pansharpening methods is of critical importance for the development of the related solutions. Unfortunately, the lack of ground-truths to be used as guidance for an objective evaluation has pushed the community to resort to either reference-based reduced-resolution indexes or to no-reference subjective quality indexes that can be applied on full-resolution datasets. In particular, the reference-based approach leverages on Wald’s protocol, a resolution degradation process that allows one to synthesize data with related ground truth. Both solutions, however, present critical shortcomings that we aim to mitigate in this work by means of an alternative no-reference full-resolution framework.

On one side we introduce a protocol, namely the reprojection protocol, which allows to handle the spectral fidelity problem. On the other side, a new index of the spatial consistency between the pansharpened image and the panchromatic band at full resolution is proposed. The experimental results show the effectiveness of the proposed approach which is confirmed also by visual inspection.

## I. INTRODUCTION

Image pansharpening is the process of merging two observations of the same scene, a low resolution multispectral (MS) component and a high resolution panchromatic (PAN) component, to generate a new multispectral image which displays both the rich spectral content of the MS and high resolution of the PAN.

By following the taxonomy proposed in [1], pansharpening methods can be roughly grouped in four main categories, component substitution (CS) [2], [3], multiresolution analysis (MRA) [4], [5], variational optimization (VO) [6], [7], and machine/deep learning (ML) [8], [9], [10]. With CS methods, the MS is transformed in a suitable domain where the PAN component replaces one of transformed band. To this end, IHS (Intensity Hue Saturation) transform, PCA (Principal Component analysis), Brovey transform, Gram-Schmidt decomposition, and others have been used. MRA methods are based on multiresolution decompositions, such as generalized Laplacian or Wavelet transforms, which allow to extract the PAN spatial details to be “injected” into the MS domain. VO methods are based on traditional optimization techniques which, through suitable constraints, ensure the pansharpened image to be spectrally consistent with the MS and spatially consistent with the PAN. Finally, ML approaches follow a data-driven paradigm where a prediction model, usually a convolutional neural network, is trained on labeled datasets, usually generated by means of Wald’s protocol [11].

Pansharpening is a very active research field, with many new methods proposed each year. Reliable quality assessment procedures are of critical importance for correctly advancing

the state of the art, and a wrong evaluation paradigm may negatively impact the design or tuning of any new solution. Unfortunately, by the very nature of pansharpening, no ground truth (GT) data are available to perform reference-based assessment. Therefore objective performance analyses rely on two complementary approaches: *i)* reference-based reduced-resolution assessment and *ii)* no-reference full-resolution assessment. Both of them present inherent limitations, which are analyzed in next Section. In this work, we propose new full-resolution quality indexes that overcome some of these problems and provide a more reliable guidance for the development of ever more accurate pansharpening methods.

In the following, Section II provides a brief critical survey on pansharpening assessment. Section III introduces the proposed approach. Section IV discusses the experimental results, and Section V draws conclusions.

## II. A REVIEW OF PANSHARPENING INDEXES

Due to the lack of ground truths, visual inspection by human experts is the ultimate benchmark for pansharpening methods. However, this is a lengthy and tedious work, and numerical indexes are essential for a viable development process. Reduced-Resolution (RR) indexes are computed, according to Wald’s protocol [11], by reducing the scale of both MS and PAN components. Then, pansharpening is performed on these rescaled data, and the original MS is used as GT to compute reference-based indexes. Instead, Full-Resolution (FR) indexes are computed on the original data and try to assess their spectral and/or spatial consistency with the pansharpened output. In a comprehensive evaluation, usually both types of indexes are considered together with visual inspection [1].

### A. Reduced-resolution assessment

In Wald’s protocol, the original MS and PAN components, called  $M$  and  $P$ , respectively, from now on, are first low-pass filtered using Gaussian kernels with band-wise Nyquist gains related to the sensor modulation transfer function (MTF). Then, they are decimated at rate  $R$ , the PAN-MS resolution ratio. The resulting RR images,  $M_{\downarrow}^{\text{lp}}$  and  $P_{\downarrow}^{\text{lp}}$ , are then used as input for pansharpening, with  $M$  playing the role of their GT. In this context, many different quality indexes can be computed to assess the mismatch between the pansharpened image and its reference, such as root mean square error, structural similarity, and so on. In particular, we will refer to some of the most popular ones for pansharpening: SAM (Spectral Angle Mapper), ERGAS (*Erreur Relative Globale Adimensionnelle de Synthèse*), and  $Q2^n$  (multiband extension of the Universal Image Quality Index, UIQI). The reader is referred to [12], [13], [14] for details.

G. Scarpa and M. Ciotola are with the Department of Electrical Engineering and Information Technology, University Federico II, Naples, Italy. e-mail: gscarpa@unina.it (G.S.), matteo.ciotola@unina.it (M.C.).

Behind its appealing simplicity, this approach hides some major hidden pitfalls that undermine its usefulness. On one hand, its accuracy depends critically on the MTF used for scaling, which may not correspond to the actual sensing conditions. More fundamentally, it relies on the arbitrary assumption that a method optimized for the RR scale will keep its good behavior at the FR scale. Experimental evidence shows this not to be the case. On the contrary, optimizing parameters for a given scale may lead to a sort of “scale overfitting”, with the perverse effect of degrading performance on a different scale. For these reasons, many recent studies focus on no-reference full-resolution quality indexes.

### B. Full-resolution no-reference assessment

Different no-reference FR quality indexes are usually employed to assess the “spectral” and the “spatial” quality of pansharpened images. In the following, let us analyze the two indexes recurring most often in the literature.

Khan’s spectral distortion index is defined [15] as

$$D_{\lambda}^{(K)} = 1 - Q2^n \left( \hat{M}^{lp}, M_{\uparrow} \right), \quad (1)$$

where  $\hat{M}$  indicates the pansharpened image,  $\hat{M}^{lp}$  its lowpass version, filtered with the estimated sensor MTF, and  $M_{\uparrow}$  the original MS component resized to PAN scale. By this definition, several shortcomings clearly appear:

- the high-pass content of the output is simply discarded;
- results depend on how the MTF is estimated;
- results depend on how the MS component is upscaled.

Item a) explains why  $D_{\lambda}^{(K)}$  is used only to assess spectral quality. The other items, however, point out further important problems, which introduce a significant degree of uncertainty for the index. For example, achieving the minimum value,  $D_{\lambda}^{(K)} = 0$ , does not ensure perfect (spectral) quality and, on the other hand, setting  $\hat{M} = \text{GT}$  (the ideal pansharpened image) does not necessarily imply  $D_{\lambda}^{(K)} = 0$ .

Similar problems can be observed in the spatial distortion index proposed in [16]

$$D_S = \frac{1}{B} \sum_{b=1}^B \left| Q(\hat{M}_b, P) - Q(M_b, P_{\downarrow}^{lp}) \right|, \quad (2)$$

where the subscript  $b$  indicates  $b$ -th band,  $P_{\downarrow}^{lp}$  is the original PAN component resized to the MS scale, and  $Q(\cdot, \cdot)$  is the UIQI distortion function. According to the definition,  $D_S$  assesses how consistent are the distortions measured at the two scales. However, results depend again on how  $P$  is down-scaled and, more important, there is no scale invariance property to ensure that such distortions *should* indeed be the same at both scales. Again,  $D_S = 0$  is no strict guarantee of quality, and  $\hat{M} = \text{GT}$  does not ensure  $D_S = 0$ .

To better substantiate such shortcomings, let us consider a simple experiment. A WorldView-3 (WV3) test image is downscaled and pansharpened, as in Wald’s protocol. In these conditions, a full-fledged GT exists (the original MS component) and all reference-based indexes can be computed. These are reported in the left part of Tab. I for some popular

	$Q2^n$	SAM	ERGAS	$D_{\lambda}^{(K)}$	$D_S$	HQNR
<b>GT</b>	1.0000	0.0000	0.0000	<b>0.0177</b>	<b>0.0490</b>	<b>0.9342</b>
<b>PRACS</b>	0.8963	7.3073	4.7028	0.0221	0.0393	0.9395
<b>MTF-GLP-FS</b>	0.9214	6.7925	<b>4.0701</b>	0.0199	0.0883	0.8935
<b>TV</b>	<b>0.9270</b>	6.6258	4.0712	0.0270	0.0825	0.8928
<b>A-PNN</b>	0.8943	<b>6.2254</b>	4.7348	<b>0.0129</b>	<b>0.0237</b>	<b>0.9637</b>
<b>EXP</b>	0.6473	7.2413	8.1472	0.0287	0.1868	0.7899

TABLE I: Objective vs subjective quality on WV3-RR.

pansharpening methods [1]. We also report (first and last rows) the indexes computed for the GT and for a simple interpolation (EXP) of the MS component. Results are as expected: GT achieves (obviously) always the optimum values, 0 or 1 depending on the index, EXP obtains almost uniformly the worst results, and all the other methods show intermediate results.

More interesting is the right part of the table, where we report also the no-reference indexes,  $D_{\lambda}^{(K)}$  and  $D_S$ , together with the Hybrid Quality with No Reference (HQNR) index [17],  $\text{HQNR} = (1 - D_{\lambda}^{(K)})(1 - D_S)$ , which summarizes them. Of course, such indexes are normally not computed in this setting, given that a GT is available, but nothing prevent using them. Results are very informative. The ideal target image, the GT, does not optimize any of the quality indexes. According to these measurements, the GT is just so-so, coming only third in terms of HQNR, much worse than the A-PNN image. Note also that the PRACS image, which has  $D_{\lambda}^{(K)}$  and  $D_S$  values close to those of the GT, has instead quite a bad quality in terms of reference-based indexes. Useful indications come, instead, for the EXP image, whose HQNR is much lower than the others.

To summarize, these no-reference indexes seem to provide indications that are reliable when the image quality is not too high, much less so at higher quality levels, when fine details count. As pansharpening methods achieve better and better results, more reliable indexes are necessary, which try to exploit effectively all the available information.

### III. PROPOSED FULL-RESOLUTION INDEXES

We now propose some new indexes for assessing the quality of pansharpening, with the aim of overcoming some limitations of traditional ones. Given the weakness of the scale-invariance assumption, we focus on full-resolution indexes, considering, as customary, different solutions for spectral and spatial quality assessment.

#### A. Reprojection protocol for spectral accuracy assessment

Let  $\mathcal{M}$  indicate a generic reference-based distortion index, such as  $Q2^n$ , SAM or ERGAS. We define the reprojection index as

$$\text{R-}\mathcal{M} = \mathcal{M} \left( \hat{M}_{\downarrow}^{lp}, M \right), \quad (3)$$

If we consider  $\mathcal{M} = Q2^n$  and neglect the complement to 1, this index looks very similar to  $D_{\lambda}^{(K)}$  defined in Eq.(1). However, in the proposed one we decimate the pansharpened image *before* computing the distortion, thereby relying only

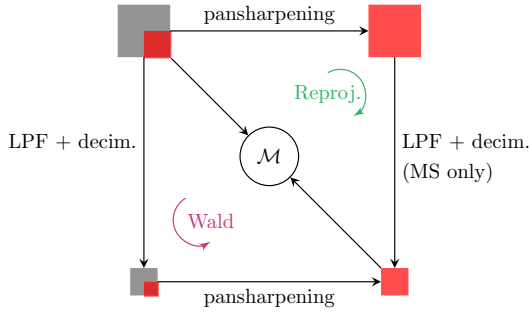


Fig. 1: Reprojection protocol (clockwise) vs Wald’s protocol (counterclockwise).  $\mathcal{M}$  is any reference-based index. In gray and red are shown the PAN and MS channels, respectively.

on pixels for which a perfectly known reference is available, the original MS component. On the contrary, with  $D_\lambda^{(K)}$ , all full-resolution pixels of the pansharpened image contribute to the distortion index, but most of them lack a solid reference, since  $M_\uparrow$  is obtained by means of an interpolation process of uncertain reliability. On the other hand, working at full-resolution is pointless, here, since detail information is compromised anyway by the low-pass filtering, and some further indexes will be necessary to assess spatial quality. Note also that reprojection indexes ensure that  $\mathcal{M}(GT_\downarrow^p, M) = 0$ , namely, that the GT achieves always the best score, as is reasonable to expect.

Another interesting comparison can be established with the reference-based reduced resolution indexes based on Wald’s protocol. Fig.1 shows pictorially the difference between these two approaches. The common starting point (top-left) is the available  $(P, M)$  pair. Indexes based on Wald’s protocol follow the counterclockwise path: decimation-pansharpening-measure. The proposed “reprojection protocol”, instead, consists in following the clockwise path: pansharpening-decimation-measure, where the actual pansharpened image is first computed, and then reprojected on the low-resolution domain for quality assessment. Eventually, in both cases, the original MS is used as a reference for any error measurement. In our proposal, however, pansharpening precedes the resolution downgrading, thereby exploiting the most valuable source of spatial information, the original PAN. Furthermore, the overall evaluation no longer depends on how the PAN is downscaled.

### B. Correlation-based spatial consistency index

As previously mentioned, the reprojection indexes are only suitable for evaluating the spectral quality, so we also propose a new index to measure the spatial quality with the aim of obtaining indications better correlated to human judgment than those provided by  $D_S$ . In particular, to assess preservation of fine-scale spatial structures, we compute the average local correlation between the pansharpened image and the reference PAN.

Let  $X_{ij}^\sigma$  indicate a  $\sigma \times \sigma$  patch of  $X$  centered on location  $(i, j)$ . We compute the field of the local correlation coefficients

between  $P$  and the  $b$ -th band of  $\hat{M}$ ,

$$\rho_{P\hat{M}}^\sigma(i, j, b) = \text{corrcoef}\left(P_{ij}^\sigma, \hat{M}(b)_{ij}^\sigma\right) \quad (4)$$

and then its average value  $\rho_{P\hat{M}}^\sigma$  over space and spectral bands. The final index is then defined as

$$D_\rho \triangleq 1 - \rho_{P\hat{M}}^\sigma \quad (5)$$

such that  $D_\rho = 0$  corresponds to perfect correlation.

Since we are interested in the fine-scale details neglected by the reprojection indexes we consider a relatively small patch size, and select  $\sigma = R = 4$ , being 4 the resolution ratio of all our data. Preliminary experiments over a large range of sizes have indeed shown that using small patches provides the most valuable indications, with the exact value of  $\sigma$  not especially critical. Under a different point of view, by choosing  $\sigma = 4$  we are studying to what extent a  $4 \times 4$  patch of any  $\hat{M}$  band can be linearly predicted from the corresponding PAN patch. Therefore,  $D_\rho$  is strictly related to the matching between the spatial layouts of  $\hat{M}$  and  $P$  at fine scale.

As for  $D_S$  or  $D_\lambda^{(K)}$ , the  $D_\rho$  index computed for  $\hat{M}=\text{GT}$  is certainly larger than zero, given the slightly different spatial layout of different bands in natural images and the complex relationship between the high resolution image and its panchromatic projection. Nonetheless, we expect good quality pansharpened images to present relatively small values of  $D_\rho$ . Eventually, more quality indexes should be observed jointly to obtain a good proxy of the perceived image quality.

## IV. EXPERIMENTAL RESULTS

The experimental validation relies on 25 methods provided in the benchmark toolbox [1] belonging to the four main categories recalled in Section I, CS (8), MRA (9), VO (3) and ML (4), plus an ideal interpolator (EXP). The dataset is composed by two WorldView-2 (WV2) and two WorldView-3 (WV3) large images, courtesy sample products of DigitalGlobe<sup>®</sup>. 20  $512 \times 512$  tiles were extracted from the WV2 images (Washington and Stockholm) and 20 from the WV3 images (Adelaide and Rio) for the experiments at full resolution. Likewise, 20+20  $2048 \times 2048$  tiles were extracted and downscaled to size  $512 \times 512$  for the experiments at reduced resolution.

### A. Reprojection indexes in the reduced-resolution space

In a first set of experiments, we used the proposed no-reference indexes in the RR domain. This allows us to compare their results with those obtained by their reference-based counterparts, which can be computed based on the available GT. In this way, we can establish how well the proposed indexes correlate with objective quality indexes.

All toolbox methods were run on all WV2 and WV3 RR tiles, and for each sample result we computed all reference-based indexes ( $Q^{2^n}$ , SAM and ERGAS) and all no reference indexes, both conventional ( $D_\lambda^{(K)}$ ,  $D_S$ ) and proposed (R- $Q^{2^n}$ , R-SAM, R-ERGAS and  $D_\rho$ ). About 10% of the sample results were excluded from the analysis as outliers (below the 0.02-quantile) mostly because some pansharpening methods failed for one reason or another. Eventually, we obtain several hundreds points in a 9-dimensional evaluation space, which enable

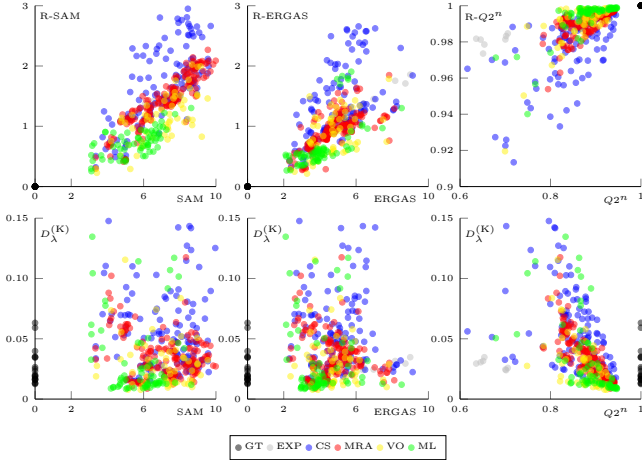


Fig. 2:  $\mathcal{M} \in \{Q2^n, \text{SAM}, \text{ERGAS}\}$  vs  $R\text{-}\mathcal{M}$  (top) and  $D_\lambda^{(K)}$  (bottom) on WorldView-2 RR dataset. Each marker is associated to a single pansharpening result on a  $512 \times 512$  tile. Black markers correspond to the ground-truth. Light gray ones (EXP) correspond to a simple interpolation. The remaining clusters correspond to the four pansharpening categories.

plenty of analyses. In Fig. 2 we show several scatter plots (only for WV2, for brevity) which allow one to appreciate the level of agreement between objective GT-based indexes and no-reference ones. In particular, we focus on spectral quality assessment and compare the proposed reprojection indexes with the conventional index  $D_\lambda^{(K)}$ .

First of all, we verify that GT points (black markers) collapse in a single corner point for all reprojections indexes but not for  $D_\lambda^{(K)}$ . More in general, the reprojection indexes correlate quite well with their reference-based counterparts, especially for SAM (spectral angle mapper) which is mostly related to spectral accuracy. Such correlation becomes even stronger when data are inspected by category. On the contrary,  $D_\lambda^{(K)}$  correlates poorly with SAM and ERGAS, and shows a reasonable agreement only with  $Q2^n$ . This is somewhat surprising, as ERGAS and SAM are more related to the spectral quality than  $Q2^n$ , which assesses correlation, mean and contrast of the compared images.

To quantify synthetically the level of agreement between reference-based and the no-reference indexes, their correlation coefficient is computed (GT scores excluded) and reported for both sensors in Tab. II. For completeness, we also report results for  $D_S$  and  $D_\rho$ , although we do not expect them to be much correlated with SAM, ERGAS and  $Q2^n$ , since the former focus on spatial accuracy while the latter are all strongly influenced by spectral quality. Overall, the proposed reprojection measures provide a consistent behavior for all indexes and both sensors.  $D_\lambda^{(K)}$  results are more scattered, although it is fair to underline that it shows good correlation with ERGAS on WV3. On the basis of these results, and lacking any theoretical reason to expect a different behavior at full resolution, we believe that the proposed reprojection approach represents an effective mean to assess the spectral distortion also at full-resolution.

	WorldView-2			WorldView-3		
	$Q2^n$	SAM	ERGAS	$Q2^n$	SAM	ERGAS
$R\text{-}\mathcal{M}$	0.62	0.72	0.61	0.33	0.61	0.55
$D_\lambda^{(K)}$	0.56	-0.11	-0.06	0.79	-0.26	0.59
$D_S$	0.29	0.39	0.19	0.19	0.38	0.08
$D_\rho$	0.49	-0.04	0.23	0.30	-0.08	0.25

TABLE II: Correlation coefficient between  $\mathcal{M} \in \{Q2^n, \text{SAM}, \text{ERGAS}\}$  and  $R\text{-}\mathcal{M}$ ,  $D_\lambda^{(K)}$ ,  $D_S$  or  $D_\rho$ .

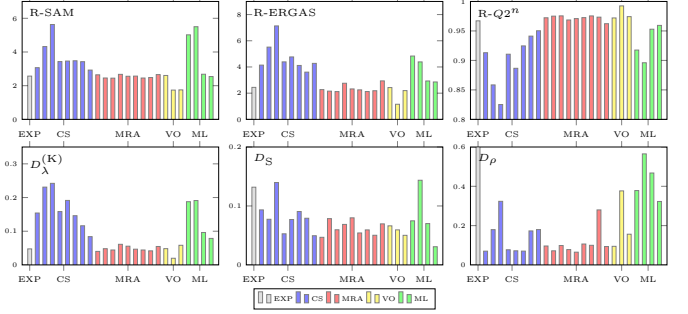


Fig. 3: Full-resolution assessment on WV3 dataset.

### B. Full-resolution assessment

To move the analysis to the target full-resolution domain, in Fig. 3 we report the numerical results of all methods according to all involved indexes, obtained on the WV3 dataset. Lacking a GT, here, only general considerations are possible. First, we observe a good agreement among all spectral indexes, reprojection measurements and  $D_\lambda^{(K)}$ , and also their good agreement with some literature findings, such as the spectral accuracy gap between MRA and CS methods [12]. Some more discrepancies, instead, are observed between the spatial indexes,  $D_\rho$  and  $D_S$ . In particular,  $D_\rho$  seems to better correlate with human experts' judgement about the good detail preservation ability of some CS solutions. Similar considerations hold for the WV2 results which are not shown for brevity.

More compelling indications, for the FR case, can be gathered only through visual inspection of results. To this end, Fig. 4 shows some FR pansharpening results for crops extracted from a single tile of the WV-3 Adelaide image. The PAN component, used as reference, is shown in the middle of two groups of results: the top-4 solutions according to  $D_S$  (left) and the top-4 according to  $D_\rho$  (right), with  $D_S$  and  $D_\rho$  computed on the whole tile. It clearly appears that images selected according to the  $D_\rho$  index ensure a better agreement with the reference in terms of spatial layout and, more in general, a better quality, with sharp contours, accurate textures, and the lack of annoying patterns such as those present in some top- $D_S$  images. Similar phenomena are observed on all other tiles, not shown for lack of space.

## V. CONCLUSIONS

We proposed new full-resolution no-reference indexes for pansharpening quality assessment. They follow the common philosophy of measuring the consistency of the full-resolution pansharpened image with the two input components, MS and PAN. Spectral quality is assessed by means of a reprojection

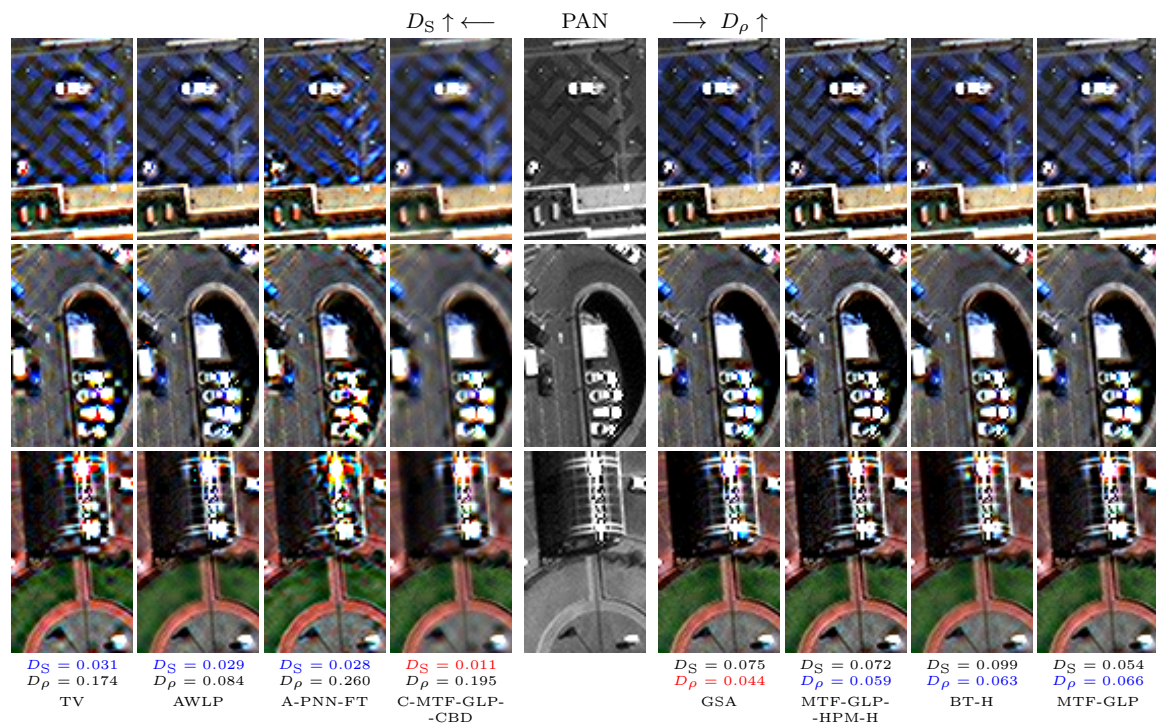


Fig. 4: Pansharpening results on crops from a FR WV3 Adelaide tile. The reference PAN is in the middle column. The four best results in terms of  $D_S$  and  $D_\rho$  are on its left and right, respectively, with best scores (in red) closer to the reference.

protocol, where the fused image is scaled back to the low-resolution domain to compare it with MS. Spatial quality, instead, is quantified by averaging the fine-scale local correlation of individual bands with the high-resolution PAN. A key qualifying aspect of the proposed indexes is the absence of any resolution downgrading of the input data, which frees the assessment from the effect of scale-dependent phenomena. Experiments on a RR dataset show that the reprojection indexes are reliable predictors of image quality as quantified by reference-based indexes, supports their use in the FR domain. On the other hand, experiments on FR data make clear that the local correlation-based index provides indications on image quality that largely agree with the judgement of human experts. The proposed approach can be readily generalized to fusion tasks other than pansharpening such as, for example, the combination of low-resolution hyperspectral and high-resolution multispectral images.

#### REFERENCES

- [1] G. Vivone, M. Dalla Mura, A. Garzelli, R. Restaino, G. Scarpa, M. O. Ulfarsson, L. Alparone, and J. Chanussot, "A new benchmark based on recent advances in multispectral pansharpening: Revisiting pansharpening with classical and emerging pansharpening methods," *IEEE Geoscience and Remote Sensing Magazine*, 2020.
- [2] J. Choi, K. Yu, and Y. Kim, "A new adaptive component-substitution-based satellite image fusion by using partial replacement," *IEEE Trans. Geosci. Remote Sens.*, vol. 49, no. 1, pp. 295–309, Jan 2011.
- [3] G. Vivone, "Robust band-dependent spatial-detail approaches for panchromatic sharpening," *IEEE Transactions on Geoscience and Remote Sensing*, vol. 57, no. 9, pp. 6421–6433, 2019.
- [4] B. Aiazzi, L. Alparone, S. Baronti, A. Garzelli, and M. Selva, "Mtf-tailored multiscale fusion of high-resolution ms and pan imagery," *Photogramm. Eng. Rem. S.*, vol. 72, no. 5, pp. 591–596, 2006.
- [5] M. Khan, J. Chanussot, L. Condat, and A. Montanvert, "Indusion: Fusion of multispectral and panchromatic images using the induction scaling technique," *IEEE Geoscience and Remote Sensing Letters*, vol. 5, no. 1, pp. 98–102, Jan 2008.
- [6] G. Vivone, M. Simões, M. Dalla Mura, R. Restaino, J. M. Bioucas-Dias, G. A. Licciardi, and J. Chanussot, "Pansharpening based on semiblind deconvolution," *IEEE Transactions on Geoscience and Remote Sensing*, vol. 53, no. 4, pp. 1997–2010, 2015.
- [7] F. Palsson, M. O. Ulfarsson, and J. R. Sveinsson, "Model-based reduced-rank pansharpening," *IEEE Geoscience and Remote Sensing Letters*, vol. 17, no. 4, pp. 656–660, 2020.
- [8] G. Masi, D. Cozzolino, L. Verdoliva, and G. Scarpa, "Pansharpening by convolutional neural networks," *Remote Sens.*, vol. 8, no. 7, p. 594, 2016.
- [9] J. Yang, X. Fu, Y. Hu, Y. Huang, X. Ding, and J. Paisley, "Pannet: A deep network architecture for pan-sharpening," in *ICCV*, Oct. 2017.
- [10] G. Scarpa, S. Vitale, and D. Cozzolino, "Target-adaptive CNN-based pansharpening," *IEEE Transactions on Geoscience and Remote Sensing*, vol. 56, no. 9, pp. 5443–5457, Sep. 2018.
- [11] L. Wald, T. Ranchin, and M. Mangolini, "Fusion of satellite images of different spatial resolution: Assessing the quality of resulting images," *Photogramm. Eng. Remote Sensing*, pp. 691–699, 1997.
- [12] G. Vivone, L. Alparone, J. Chanussot, M. D. Mura, A. Garzelli, G. A. Licciardi, R. Restaino, and L. Wald, "A critical comparison among pansharpening algorithms," *IEEE Trans. Geosci. Remote Sens.*, vol. 53, no. 5, pp. 2565–2586, May 2015.
- [13] L. Wald, "Data fusion: Definitions and architectures—fusion of images of different spatial resolutions," *Les Presses de l'École des Mines*, 2002.
- [14] A. Garzelli and F. Nencini, "Hypercomplex quality assessment of multi/hyperspectral images," *Geoscience and Remote Sensing Letters, IEEE*, vol. 6, no. 4, pp. 662–665, Oct 2009.
- [15] M.M.Khan, L.Alparone, and J.Chanussot, "Pansharpening quality assessment using the modulation transfer functions of instruments," *IEEE Trans. Geosci. Remote Sens.*, vol. 47, no. 11, pp. 3880–3891, 2009.
- [16] L. Alparone, B. Aiazzi, S. Baronti, A. Garzelli, F. Nencini, and M. Selva, "Multispectral and panchromatic data fusion assessment without reference," *Photogramm. Eng. Rem. S.*, vol. 74, no. 2, pp. 193–200, 2008.
- [17] B. Aiazzi, L. Alparone, S. Baronti, R. Carlà, A. Garzelli, and L. Santurri, "Full scale assessment of pansharpening methods and data products," in *Proc. SPIE*, vol. 9244, 2014, pp. 1–12.